

Structure-based design of novel quinoxaline-2-carboxylic acids and analogues as Pim-1 inhibitors

Bruno Oyallon, Marie Brachet-Botineau, Cédric Logé, Pascal Bonnet, Mohamed Souab, Thomas Robert, Sandrine Ruchaud, Stéphane Bach, Pascal Berthelot, Fabrice Gouilleux, et al.

▶ **To cite this version:**

Bruno Oyallon, Marie Brachet-Botineau, Cédric Logé, Pascal Bonnet, Mohamed Souab, et al.. Structure-based design of novel quinoxaline-2-carboxylic acids and analogues as Pim-1 inhibitors. European Journal of Medicinal Chemistry, 2018, 154, pp.101-109. 10.1016/j.ejmech.2018.04.056 . hal-03408667

HAL Id: hal-03408667
https://hal.science/hal-03408667

Submitted on 3 Nov 2021

HAL is a multi-disciplinary open access archive for the deposit and dissemination of scientific research documents, whether they are published or not. The documents may come from teaching and research institutions in France or abroad, or from public or private research centers.

L'archive ouverte pluridisciplinaire **HAL**, est destinée au dépôt et à la diffusion de documents scientifiques de niveau recherche, publiés ou non, émanant des établissements d'enseignement et de recherche français ou étrangers, des laboratoires publics ou privés.

European Journal of Medicinal Chemistry 154 (2018) 101–109

Contents lists available at ScienceDirect

European Journal of Medicinal Chemistry

journal homepage: http://www.elsevier.com/locate/ejmech

Research paper

Structure-based design of novel quinoxaline-2-carboxylic acids and analogues as Pim-1 inhibitors

Bruno Oyallon [a], Marie Brachet-Botineau [b, c], Cédric Logé [d], Pascal Bonnet [e], Mohamed Souab [f], Thomas Robert [f], Sandrine Ruchaud [f], Stéphane Bach [f], Pascal Berthelot [g], Fabrice Gouilleux [b], Marie-Claude Viaud-Massuard [a], Caroline Denevault-Sabourin [a, *]

[a] EA GICC - ERL 7001 CNRS « Groupe Innovation et Ciblage Cellulaire », Team Innovation Moléculaire et Thérapeutique, University of Tours, F-37200, Tours, France
[b] CNRS ERL7001 LNOx « Leukemic Niche and RedOx Metabolism » - EA GICC, University of Tours, F-37000, Tours, France
[c] CHRU de Tours, Service d'Hématologie Biologique, F-37044, Tours, France
[d] Université de Nantes, Nantes Atlantique Universités, Département de Chimie Thérapeutique, Cibles et Médicaments des Infections et du Cancer, IICIMED-EA1155, Institut de Recherche en Santé 2, F-44200, Nantes, France
[e] UMR University of Orléans-CNRS 7311, Institut de Chimie Organique et Analytique (ICOA), University of Orléans, F-45067, Orléans, France
[f] Sorbonne Universités, USR3151 CNRS/UPMC, Plateforme de criblage KISSf (Kinase Inhibitor Specialized Screening Facility), Station Biologique, Place Georges Teissier, F-29688, Roscoff, France
[g] UMR-S 1172 - JPArc - Centre de Recherche Jean-Pierre AUBERT Neurosciences et Cancer, University of Lille, Inserm, CHU Lille, F-59000, Lille, France

ARTICLE INFO

Article history:
Received 27 February 2018
Received in revised form
20 April 2018
Accepted 28 April 2018
Available online 11 May 2018

Keywords:
Quinoxaline
Pim-1
Kinase inhibitor
Anticancer targeted therapy

ABSTRACT

We identified a new series of quinoxaline-2-carboxylic acid derivatives, targeting the human proviral integration site for Moloney murine leukemia virus-1 (*Hs*Pim-1) kinase. Seventeen analogues were synthesized providing useful insight into structure-activity relationships studied. Docking studies realized in the ATP pocket of *Hs*Pim-1 are consistent with an unclassical binding mode of these inhibitors. The lead compound **1** was able to block *Hs*Pim-1 enzymatic activity at nanomolar concentrations (IC_{50} of 74 nM), with a good selectivity profile against a panel of mammalian protein kinases. *In vitro* studies on the human chronic myeloid leukemia cell line KU812 showed an antitumor activity at micromolar concentrations. As a result, compound **1** represents a promising lead for the design of novel anticancer targeted therapies.

© 2018 Elsevier Masson SAS. All rights reserved.

1. Introduction

Proviral integration site for Moloney murine leukemia virus (Pim) kinases belong to a small family of constitutively activated proto-oncogenic serine/threonine protein kinases, constituted of three isoforms: Pim-1, Pim-2 and Pim-3 [1]. These oncoproteins control many cellular functions like cell cycle regulation, apoptosis, cell survival, proliferation and differentiation [2,3], and are overexpressed in a large number of human cancer types, such as hematopoietic malignancies [4,5] and solid cancers (*e. g.* bladder [6], prostate [7], breast [8] or oral cancers [9]). These kinases are positive regulators of cell cycle progression at G1/S and G2/M checkpoints, and inhibit apoptosis, acting as oncogenic survival factors [10]. Interestingly, it has been demonstrated that *Pim1*$^{-/-}$2$^{-/-}$3$^{-/-}$ triple knockout mice were viable and fertile, which make these kinases very interesting for targeted cancer therapies [11].

Recently, Pim-1 has been shown to play a significant role in cancer stem cells growth, and in resistance to chemotherapy drugs, promoting multiple drug resistance [12,13]. This kinase is thus considered as a relevant target for cancer therapy and a large variety of small molecule inhibitors have been developed [14–18].

Abbreviations: IC50, 50% inhibitory concentration; SAR, structure-activity relationships; Pim, proviral integration site of Moloney murine leukemia virus; CML, chronic myeloid leukemia; DYRK1A, dual specificity tyrosine phosphorylation regulated kinase 1A; CDK, cyclin-dependent kinase; Haspin, haploid germ cell-specific nuclear protein kinase; CLK1, CDC2-like kinase 1; CK1, casein kinase 1; GSK3, glycogen synthase kinase 3.

* Corresponding author. Department of Innovation Moléculaire et Thérapeutique, EA GICC - ERL 7001 CNRS, University of Tours, 31 avenue Monge, F-37200, Tours, France.
E-mail address: caroline.sabourin@univ-tours.fr (C. Denevault-Sabourin).

https://doi.org/10.1016/j.ejmech.2018.04.056
0223-5234/© 2018 Elsevier Masson SAS. All rights reserved.

Many of these Pim-1 kinase inhibitors demonstrated significant *in vitro* activity in cancer cell lines and in different *in vivo* tumor xenograft models, and clinical trials are currently ongoing for the most promising candidates [14,18].

A remarkable characteristic of Pim-1 active site in comparison to other protein kinases is the presence of an original hinge region (region containing backbone peptide atoms that forms hydrogen bond interactions (H-bonds) with the adenine moiety of ATP). Indeed, this region contains a proline residue (Pro123), which has no H-bond donor property and precludes the formation of one of the conserved H-bond involving the hinge backbone and the ATP adenine ring, as it can be observed in other kinases. Thus, Pim-1 bounds ATP *via* only one hinge H-bond between the ATP adenine amino moiety and the backbone carbonyl of glutamate 121 (Glu121). Moreover, the insertion in the hinge of a valine (Val126), absent in other kinases, changes the hinge conformation, enlarging the catalytic pocket. This unique feature can be exploited for the design of selective inhibitors [19].

The vast majority of Pim-1 inhibitors mainly act as ATP competitive inhibitors, targeting the ATP-binding pocket. They can be classified into two categories: ATP-mimetics, which bind to the Glu121 residue of the hinge region, and non-ATP mimetics, which interact with the ATP binding cleft in a different manner from ATP [20].

In a continuing effort to develop new small molecule inhibitors with anticancer properties, our laboratory has been recently focusing on the study of new inhibitors of the signal transducer and activator of transcription 5 (STAT5) activation and expression and their interest in chronic myeloid leukemia (CML) [21]. Indeed, the STAT family transcription factors are commonly activated in cancer by upstream mutations or cell surface signaling molecules. It has been demonstrated that the Pim kinases are induced by the STAT family transcription factors (particularly STAT 3/5) [14]. Regarding the potential of Pim-1 as target in cancer therapy and particularly in leukemia [22,23], we decided to further explore the STAT signaling pathway, by developing new Pim-1 kinase specific inhibitors. In this purpose, we first performed a target-based approach, by realizing a focused *in vitro* screening of our chemical library on a limited panel of kinases, comprising *Homo sapiens* Pim-1 (*Hs*Pim-1), allowing the identification of the quinoxaline-2-carboxylic acid **1** as a new lead compound (Fig. 1). This molecule was able to inhibit the *in vitro* enzymatic activity of *Hs*Pim-1 with an IC_{50} of 74 nM.

Docking studies, using program GOLD (GOLD version 4.0; CCDC, Cambridge, UK), were performed to understand the binding interactions between the lead compound **1** and the ATP pocket of *Hs*Pim-1 (PDB ID 3A99) (Fig. 2). Data analysis suggests that the carboxylate group of this molecule can form a key salt bridge with the protonated amino group side chain of catalytic Lys67, as it has already been described in other Pim-1 inhibitors [24,25], and shares also a H-bond interaction with the backbone NH of Asp186 belonging to the DFG motif. Additionally, an H-bond interaction between the 3-hydroxyphenyl moiety and the carboxylate group of residue Asp186 can be observed. These studies suggested that compound **1** could act as an ATP competitive inhibitor, with a non-ATP mimetic binding mode.

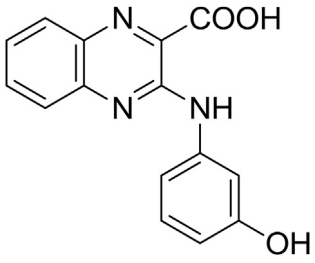


Fig. 1. Chemical structure of compound **1**.

Sixteen new analogues were then synthesized, exploiting the unique sequence of *Hs*Pim-1 ATP-binding cleft.

We report herein the design, synthesis, structure-activity relationships (SAR) and *in vitro* evaluations of this new class of Pim-1 inhibitors.

2. Chemistry

The preparation of quinoxaline-2-carboxylic acids **1**, **5c-e**, and **5h-i** and potassium carboxylate salts **5b**, and **5g** was performed as shown in Scheme 1 by amination of the intermediate ethyl 3-chloroquinoxaline-2-carboxylate **3** with the appropriate amine derivatives.

The synthesis of ethyl 3-chloroquinoxaline-2-carboxylate **3** was achieved in two steps from commercial *o*-phenylenediamine according to literature procedures [26,27] (Scheme 1). First, the *o*-phenylenediamine was condensed with diethyl 2-oxomalonate in the presence of citric acid (3 mol%) at room temperature in ethanol to give ester **2**, which was then chlorinated using *N*,*N*-dimethylformamide (DMF) as a catalyst in refluxing phosphorous oxychloride, affording the intermediate **3** in quantitative yield.

Access to quinoxaline-2-carboxylic acids, and potassium carboxylate salts was then performed using a two-step synthetic pathway. Thus, intermediate **3** undergoes initial nucleophilic aromatic substitution with the appropriate amine in presence of *p*-TSA as a catalyst in refluxing absolute ethanol to give esters **4a-f** and **4h-i** [28]. For compound **4f**, a supplementary step of *tert*-butyloxycarbonyl (Boc) group deprotection, using trifluoroacetic acid in dichloromethane (DCM), was necessary to obtain the derivative **4g**. Then, hydrolysis of the intermediate ethyl esters **4a-c**, **4e**, and **4g-i** with potassium carbonate in refluxing 80% aqueous methanol was performed. The potassium salts **5b** and **5g** were thus obtained without any treatment. A subsequent acidification with a citric acid aqueous solution was realized to afford acids **1**, **5c-e**, and **5h-i**.

Ester **4d** was saponified using a 10% aqueous sodium hydroxide solution in refluxing ethanol, leading, after acidification with a citric acid aqueous solution, to the corresponding carboxylic acid **5d**.

Finally, synthesis of the carboxamide **6** was achieved from acid **5c**, using *N*-methylmorpholine and ethyl chloroformate in dichloromethane at 0 °C, followed by the addition of a 28% ammonium hydroxide solution.

3. Results and discussion

3.1. Enzymatic assays

3.1.1. Pim-1 enzymatic activity inhibition

Compounds were first evaluated for their efficacy to inhibit the *in vitro* enzymatic activity of *Hs*Pim-1, using a luminescence-based kinase assay [29]. Compounds that displayed *Hs*Pim-1 $IC_{50} > 10\ \mu M$ were considered inactive.

To get closer insight into the potential binding mode of our compounds within the ATP binding pocket of *Hs*Pim-1, we first decided to structurally vary the substitution patterns of the quinoxaline scaffold of **1** in position 3 (Table 1). Docking analysis revealed that the hydroxyl moiety of the phenyl ring in this position could be able to form an H-bond interaction with the carboxylate side chain of residue Asp186 of the *Hs*Pim-1 ATP binding pocket. Interestingly, it appears that position of the hydroxyl group on the phenyl ring strongly modulates compound activity, since modification from meta (**1**) to para (**5e**) or ortho (**5i**) position reduced

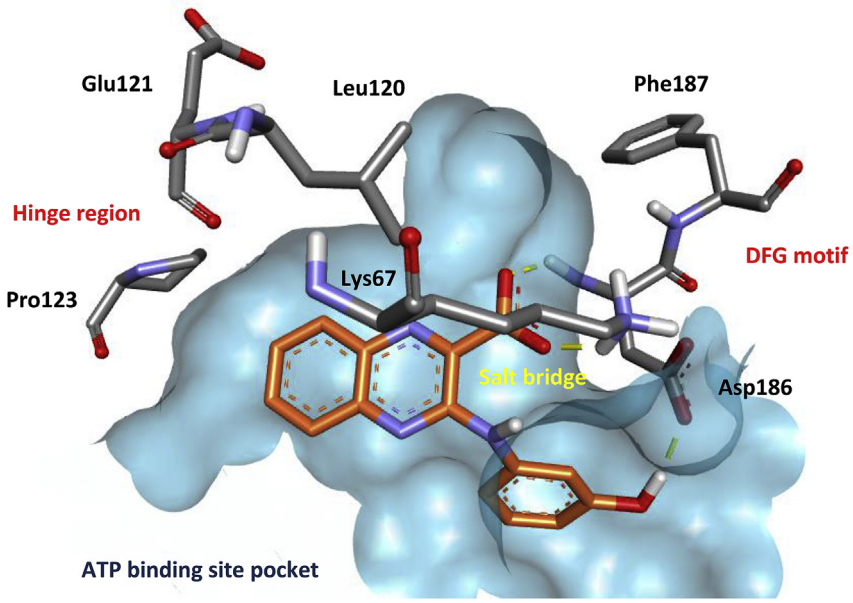
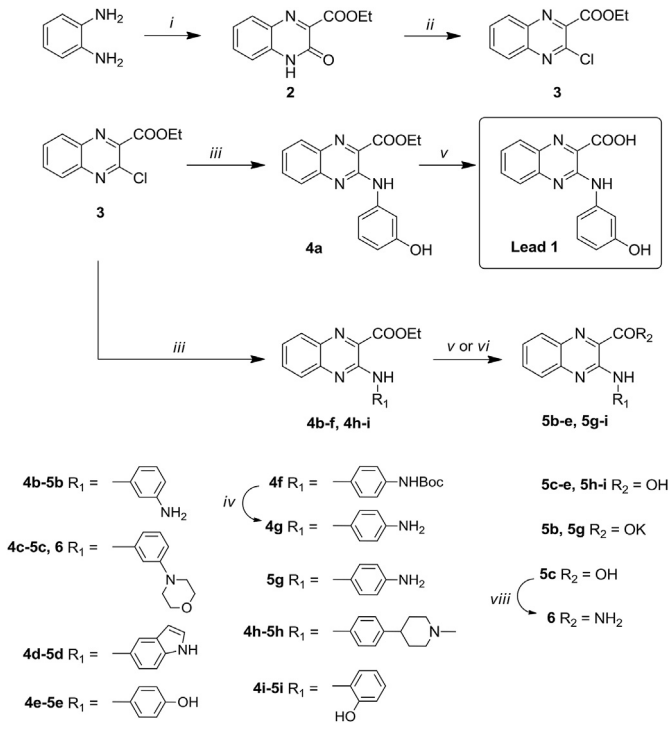


Fig. 2. Binding pose found by the docking program GOLD for compound **1** into the ATP pocket of Pim-1 (PDB ID 3A99). Hydrogen bonds are indicated as yellow lines. (For interpretation of the references to colour in this figure legend, the reader is referred to the Web version of this article.)



Scheme 1. Reagents and conditions: (*i*) diethyl 2-oxomalonate (1 eq), citric acid (3 mol %), EtOH, rt, 10 min, 79%; (*ii*) DMF (cat.), $POCl_3$, 0 °C, and then reflux, 30 min, 100%; (*iii*) amine (1.1–3 eq), *p*-toluenesulfonic acid (cat.), EtOH, reflux, 20–112 h, 32–93%; (*iv*) TFA (20%), DCM, rt, 6 h, 96%; (*v*) K_2CO_3 (1–4 eq), MeOH/H_2O (4/1), reflux, 4 h, 49–100%; (*vi*) NaOH (10%), EtOH, reflux, 18 h, 41%; (*vii*) ClCOOEt (1.5 eq), NMM (2 eq), DCM, 0 °C, 1 h, and NH_4OH, rt, overnight, 100%.

significantly the inhibitory potency (Table 1, entries 2, 11, and 17). Thus, compounds **5e** and **5i** maintained a submicromolar activity on *Hs*Pim-1 (IC_{50} of 0.29 μM and 0.76 μM, respectively) but were less potent (4-fold, 10-fold, respectively) than lead compound **1** (IC_{50} of 74 nM).

Surprisingly, the replacement of the hydroxyl moiety of compound **1** by an amino group, able to form an H-bond with Asp186, led to a significant loss of potency (**5b**, IC_{50} of 2.80 μM, 38-fold lower). However, as expected, the substitution by a morpholino group, suppressing the formation of an H-bond, was not favorable for the activity, as shown by derivative **5c** (IC_{50} of 1.01 μM). Again, the para substitution on the phenyl ring was deleterious for the activity, as shown by derivative **5g** which was >3.5-fold less active than its "meta" analogue **5b**, and by the inactive compound **5h** (Table 1, entries 4, 13 and 15).

Finally, replacement of the 3-hydroxyphenyl moiety of compound **1** by an 1*H*-indol-5-yl group (**5d**) led to a drastic loss of potency (Table 1, entry 9).

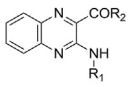
Docking analysis also suggested that the carboxylate function in position 2 of the quinoxaline scaffold of compound **1** was crucial for the activity, establishing, notably, a key salt bridge with the catalytic Lys67. However, carboxylic acids are known to be responsible for limited permeability across biological membranes, metabolic instability, and potential adverse effects [30]. To circumvent these issues, and to confirm the results of the modeling studies, we evaluated ethyl ester derivatives (**4a-e** and **4g-i**) of all synthesized acids and carboxylate salts, and we replaced the acid group of compound **5c** by a carboxamide isosteric moiety (**6**). Both ester and carboxamide functions are not able to form a salt bridge like the carboxylic acid group, resulting in a complete loss of *Hs*Pim-1 enzymatic activity inhibition (Table 1, entries 1, 3, 5, 7, 8, 10, 12, 14 and 16), highlighting the highly critical role of this type of interaction in position 2 of the quinoxaline ring.

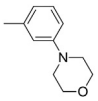
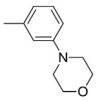
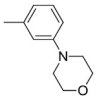
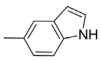
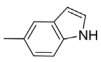
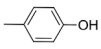
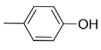
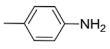
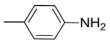
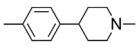
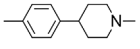
3.1.2. Selectivity over a panel of mammalian protein kinases

A selectivity profile of the most active *Hs*Pim-1 inhibitors was performed. In that purpose, most promising candidates were further evaluated in an expanded panel of mammalian protein kinases such as *Rn*DYRK1A, *Hs*CDK2/CyclinA, *Hs*CDK9/CyclinT, *Hs*Haspin, *Mm*CLK1, *Ssc*CK1δ/ε and *Ssc*GSK3α/β. Inhibition values were determined using a luminescence-based kinase assay [29].

Similar inhibition trends were observed with 6 of the mammalian kinases tested (*Hs*CDK2/CyclinA, *Hs*CDK9/CyclinT, *Hs*Haspin, *Mm*CLK1, *Ssc*CK1δ/ε and *Ssc*GSK3α/β), with $IC_{50} > 10$ μM

Table 1
Enzymatic assays on *Hs*Pim-1.



Entry	Compd	R_1	R_2	*Hs*Pim-1 IC_{50} (μM)[a]
1	**4a**		OEt	>10
2	**1**		OH	0.074
3	**4b**		OEt	>10
4	**5b**		OK	2.80
5	**4c**		OEt	>10
6	**5c**		OH	1.01
7	**6**		NH_2	>10
8	**4d**		OEt	>10
9	**5d**		OH	>10
10	**4e**		OEt	>10
11	**5e**		OH	0.29
12	**4g**		OEt	>10
13	**5g**		OK	>10
14	**4h**		OEt	>10
15	**5h**		OH	>10
16	**4i**		OEt	>10
17	**5i**		OH	0.76
18	**Staurosporine**			0.031

[a] Values are a mean of $n \geq 3$ independent experiments. *Hs*: *Homo sapiens*.

in every case, for each compound evaluated, suggesting an interesting selectivity profile against these potential off-target kinases (Table 2). Notably, we observed >130-fold differences between IC_{50} values for *Hs*Pim-1 over these mammalian kinases for our lead inhibitor **1**.

In contrast, quinoxalines **1**, **5b**, **5e** and **5i** displayed a micromolar to submicromolar inhibition of *Rn*DYRK1A (Table 2, entries 1, 2, 4 and 5). Lead **1** exhibited nevertheless an IC_{50} value at least 3.5-fold higher for *Rn*DYRK1A than for *Hs*Pim-1. Interestingly, compound **5c**, despite a less potent activity profile against *Hs*Pim-1, was more than 10-fold selective with respect to this kinase (Table 2, entry 3).

3.2. In vitro cell-based assays

Most active *Hs*Pim-1 inhibitors were then tested *in vitro* on the human CML cell line KU812, overexpressing Pim-1. Cytotoxic effects were evaluated using a MTT assay, and living cells were also counted with the trypan blue dye exclusion method.

As expected, a same trend was observed between *Hs*Pim-1 enzymatic activity inhibition and *in vitro* cytotoxic potency. Indeed, quinoxalines with a good level of activity on *Hs*Pim1 (IC_{50} of 0.074–2.80 μM) also exhibited *in vitro* cytotoxic effects on KU812 cell line with EC_{50} values ranging from 38.9 ± 3.4 μM to 177.5 ± 13.1 μM (Table 2). Moreover, the best *Hs*Pim-1 inhibitor **1** (IC_{50} of 74 nM), was also the most cytotoxic compound (EC_{50} of 38.9 ± 3.4 μM).

4. Conclusion

In this study, we identified a new series of quinoxaline-2-carboxylic acids and analogues, exhibiting a potent activity against the *Hs*Pim-1 oncoprotein. Among the 17 compounds synthesized, 5 significantly blocked *Hs*Pim-1 with IC_{50} values in the submicromolar to low micromolar range. In particular, lead compound **1** showed the best inhibitory effect against *Hs*Pim-1, with an IC_{50} value of 74 nM. SAR in positions 2 and 3 of the quinoxaline scaffold confirmed the molecular modeling studies, highlighting the crucial role of the carboxylic acid function in position 2 for the *Hs*Pim-1 inhibitory activity of these compounds. *In vitro* studies of the 5 most potent inhibitors on the human CML cell line KU812, confirmed their interest, with antitumor activities at micromolar concentrations.

This series of compounds, and particularly lead **1**, could therefore represent new attractive drug candidates for extending further pharmacomodulation studies in a way to improve their potency and selectivity profile.

5. Experimental section

5.1. General remarks

All solvents were anhydrous reagents from commercial sources. Unless otherwise noted, all chemicals and reagents were obtained commercially and used without purification. Microwave heating was carried out with a single-mode Initiator Alstra (Biotage) unit. Melting points (Mp) were determined on a Stuart capillary apparatus and are uncorrected. High-resolution mass spectra (HRMS) were performed in positive mode with an ESI source on a Q-TOF mass spectrometer (Bruker maXis) with an accuracy tolerance of 2 ppm. NMR spectra were recorded at 300 MHz (^1H) or 75 MHz (^{13}C) on a Bruker Avance (300 MHz) spectrometer. The chemical shifts are reported in parts per million (ppm, δ) relative to residual deuterated solvent peaks. The abbreviations s = singlet, d = doublet, t = triplet, q = quadruplet, m = multiplet and bs = broad signal were used throughout. Known compounds were prepared according to literature procedures: *tert*-butyl (3-aminophenyl)carbamate, and *tert*-butyl (4-aminophenyl)carbamate [31], 4-(1-methylpiperidin-4-yl)aniline [32].

Table 2
Kinase selectivity profile and cell-based assays of most active quinoxalines.



Entry	Cpd	R_1	R_2	Kinase enzymatic IC_{50} (μM)[a]								EC_{50} (μM)[a]
				*Hs*Pim-1	*Rn*DYRK1A	*Hs*CDK2/CyclinA	*Hs*CDK9/CyclinT	*Hs* Haspin	*Mm* CLK1	*Ssc* CK1δ/ε	*Ssc* GSK3α/β	KU 812[b]
1	**1**		H	0.074	0.27	>10	>10	>10	>10	>10	>10	38.9 ± 3.4
2	**5b**		K	2.80	1.67	>10	>10	>10	>10	>10	>10	63.8 ± 1.9
3	**5c**		H	1.01	>10	>10	>10	>10	>10	>10	>10	57.3 ± 6.1
4	**5e**		H	0.29	0.098	>10	>10	>10	>10	>10	>10	41.7 ± 3.7
5	**5i**		H	0.76	0.74	>10	>10	>10	>10	>10	>10	177.5 ± 13.1
6	**Imatinib mesylate**			ND	ND	ND	ND	ND	ND	ND	ND	0.6 ± 0.02

Rn: *Rattus norvegicus*, *Hs*: *Homo sapiens*, *Mm*: *Mus musculus*, *Ssc*: *Sus scrofa*, DYRK1A: dual specificity tyrosine phosphorylation regulated kinase 1A, CDK: cyclin-dependent kinase, Haspin: haploid germ cell-specific nuclear protein kinase, CLK1: CDC2-like kinase 1, CK1: casein kinase 1, GSK3: glycogen synthase kinase 3, ND: not determined.
[a] Values are a mean of $n \geq 3$ independent experiments.
[b] Cells were treated with concentrations ranging from 100 nM to 50 μM for 48 h. Cell viability was then determined by MTT assays, and EC_{50} values were calculated using Graphpad PRISM 7 software (n = 3 in triplicate; data are the mean ± SEM).

5.2. Chemistry

5.2.1. Ethyl 3-oxo-3,4-dihydroquinoxaline-2-carboxylate (**2**)

A mixture of *o*-phenylenediamine (708 mg, 6.55 mmol), diethyl 2-oxomalonate (1.14 g, 6.55 mmol) and citric acid (41 mg, 0.20 mmol) in ethanol (13 mL) was stirred magnetically at room temperature for 10 min. Ethanol was then evaporated under reduced pressure, and the residue was stirred with crushed ice for 5 min, filtered and dried under vacuum to give compound **2** (1.13 g, 79%) as a beige solid.

Mp 168.8 °C. ^{1}H NMR (300 MHz, $CDCl_3$) δ 12.85 (bs, 1H, NH), 7.97 (dd, 1H, *J* = 8.1, 1.2 Hz), 7.64 (dd, 1H, *J* = 8.1, 7.2, 1.2 Hz), 7.48 (dd, 1H, *J* = 8.1, 1.2 Hz), 7.42 (dd, 1H, *J* = 8.1, 7.2, 1.2 Hz), 4.56 (q, 2H, *J* = 7.2 Hz, CH_2), 1.49 (t, 3H, *J* = 7.2 Hz, CH_3). ^{13}C NMR (75 MHz, $CDCl_3$) δ 163.4, 154.6, 148.4, 132.8, 132.2, 132.1, 130.2, 125.0, 116.5, 62.6, 14.2.

5.2.2. Ethyl 3-chloroquinoxaline-2-carboxylate (**3**)

Into a dry three-neck round bottom flask was introduced compound **2** (218 mg, 1.00 mmol) in phosphorous oxychloride (2 mL) at ice bath temperature. Dimethylformamide (0.1 mL) was then added at 0 °C and the reaction mixture was refluxed for 30 min. After cooling, the resulting mixture was diluted with ethyl acetate and washed with a 10% sodium hydroxide solution (2 × 5 mL), and brine (2 × 10 mL). The combined organic layers were dried over $MgSO_4$, filtered, and evaporated under reduced pressure to obtain derivative **3** (237 mg, 100%) as a beige solid.

Mp 46.4 °C. ^{1}H NMR (300 MHz, $CDCl_3$) δ 8.18 (m, 1H), 8.07 (m, 1H), 7.92–7.81 (m, 2H), 4.58 (q, 2H, *J* = 7.2 Hz, CH_2), 1.49 (t, 3H, *J* = 7.2 Hz, CH_3). ^{13}C NMR (75 MHz, $CDCl_3$) δ 163.9, 144.7, 143.9, 142.2, 139.7, 132.6, 131.0, 129.6, 128.3, 63.0, 14.1.

5.2.3. Ethyl 3-((3-hydroxyphenyl)amino)quinoxaline-2-carboxylate (***4a***)

Method A: a solution of compound **3** (1.11 g, 4.70 mmol), 3-aminophenol (622 mg, 5.70 mmol) and *p*-TSA, as a catalyst, in absolute ethanol (40 mL) was refluxed for 110 h. Ethanol was then evaporated under reduced pressure, and the resulting residue was purified by silica column chromatography using cyclohexane with ethyl acetate gradient (0–50%) as eluent to give the desired compound **4a** (1.0 g, 69%) as a red powder.

Mp 233.3 °C. ^{1}H NMR (300 MHz, DMSO-d6) δ 10.08 (bs, 1H, NH), 9.52 (bs, 1H, OH), 7.99 (dd, 1H, *J* = 8.4, 0.6 Hz), 7.85–7.75 (m, 2H), 7.61–7.54 (m, 2H), 7.24–7.14 (m, 2H), 6.51 (dd, 1H, *J* = 7.4, 2.4, 1.5 Hz), 4.48 (q, 2H, *J* = 7.2 Hz, CH_2), 1.41 (t, 3H, *J* = 7.2 Hz, CH_3). ^{13}C NMR (75 MHz, DMSO-d6) δ 166.1, 158.3, 148.8, 142.4, 140.7, 136.0, 133.4, 132.7, 130.0 (2 × C), 126.7, 126.6, 111.1, 110.6, 107.3, 62.8, 14.5.

5.2.4. Ethyl 3-((3-aminophenyl)amino)quinoxaline-2-carboxylate (***4b***)

The title compound was synthesized according to the general method A from compound **3** (330 mg, 1.40 mmol) and *tert*-butyl (3-aminophenyl)carbamate (312 mg, 1.50 mmol) in absolute ethanol (10 mL). The reaction mixture was refluxed for 110 h. Compound **4b** was obtained (139 mg, 32%) as a red powder.

Mp 207.7 °C. ^{1}H NMR (300 MHz, DMSO-d6) δ 10.00 (bs, 1H, NH), 7.97 (d, 1H, *J* = 8.1 Hz), 7.81–7.77 (m, 2H), 7.58–7.51 (m, 1H), 7.26 (bs, 1H), 7.09–6.97 (m, 2H), 6.32 (m, 1H), 5.17 (bs, 2H, NH_2), 4.48 (q, 2H, *J* = 7.2 Hz, CH_2), 1.41 (t, 3H, *J* = 7.2 Hz, CH_3). ^{13}C NMR (75 MHz, DMSO-d6) δ 166.1, 149.7, 149.0, 142.6, 140.3, 135.9, 133.3, 132.5, 130.0, 129.7, 126.7, 126.4, 109.7, 108.2, 105.8, 62.8, 14.5.

5.2.5. Ethyl 3-((3-morpholinophenyl)amino)quinoxaline-2-carboxylate (***4c***)

The title compound was synthesized according to the general method A from compound **3** (361 mg, 1.53 mmol) and 3-morpholinoaniline (299 mg, 1.68 mmol) in absolute ethanol (10 mL). The reaction mixture was refluxed for 110 h. Compound **4c** was obtained (439 mg, 76%) as an orange powder.

Mp 170.6 °C. ^{1}H NMR (300 MHz, DMSO-d6) δ 10.09 (bs, 1H, NH), 7.98 (d, 1H, *J* = 8.1 Hz), 7.87–7.70 (m, 2H), 7.67–7.47 (m, 2H), 7.34 (d, 1H, *J* = 7.8 Hz), 7.24 (t, 1H, *J* = 8.1 Hz), 6.71 (d, 1H, *J* = 7.8 Hz), 4.48 (q, 2H, *J* = 6.9 Hz, CH_2), 3.77 (m, 4H, 2 × CH_2O morpholine), 3.16 (m, 4H, 2 × CH_2N, morpholine), 1.41 (t, 3H, *J* = 6.9 Hz, CH_3). ^{13}C NMR (75 MHz, DMSO-d6) δ 166.0, 152.2, 148.9, 142.4, 140.4, 136.0, 133.5, 132.6, 130.0, 129.8, 126.7 (2 × C), 111.5, 110.7, 107.1, 66.6 (2 × C), 62.8, 48.9 (2 × C), 14.5.

*5.2.6. Ethyl 3-((1H-indol-5-yl)amino)quinoxaline-2-carboxylate (**4d**)*

The title compound was synthesized according to the general method A from compound **3** (237 mg, 1.00 mmol) and 5-aminoindole (397 mg, 3.00 mmol) in absolute ethanol (10 mL). The reaction mixture was refluxed for 36 h. Compound **4d** was obtained (245 mg, 73%) as a red powder.

Mp 204.7 °C. ^{1}H NMR (300 MHz, $CDCl_3$) δ 10.24 (bs, 1H, NH), 8.80 (bs, 1H, NH), 8.26 (s, 1H, indolyl), 8.00 (dd, 1H, J = 8.4, 0.9 Hz), 7.77 (dd, 1H, J = 8.4, 0.9 Hz), 7.66 (dd, 1H, J = 8.4, 6.9, 0.9 Hz), 7.50–7.38 (m, 3H), 7.23 (t, 1H, J = 2.4 Hz, indolyl), 6.56 (bs, 1H, indolyl), 4.60 (q, 2H, J = 7.2 Hz, CH_2), 1.53 (t, 3H, J = 7.2 Hz, CH_3). ^{13}C NMR (75 MHz, $CDCl_3$) δ 166.4, 150.0, 143.6, 136.2, 133.0, 132.8, 131.5, 130.6, 130.1, 128.1, 126.6, 125.4, 125.1, 117.2, 112.8, 111.2, 102.6, 62.9, 14.3.

*5.2.7. Ethyl 3-((4-hydroxyphenyl)amino)quinoxaline-2-carboxylate (**4e**)*

The title compound was synthesized according to the general method A from compound **3** (302 mg, 1.28 mmol) and 4-aminophenol (418 mg, 3.83 mmol) in absolute ethanol (16 mL). The reaction mixture was refluxed for 20 h. Compound **4e** was obtained (155 mg, 39%) as a red powder.

Mp 231.8 °C. ^{1}H NMR (300 MHz, DMSO-d6) δ 9.84 (bs, 1H, NH), 9.30 (bs, 1H, OH), 7.94 (d, 1H, J = 8.1 Hz), 7.80–7.60 (m, 4H), 7.51 (m, 1H), 6.80 (d, 2H, J = 8.7 Hz), 4.47 (q, 2H, J = 7.2 Hz, CH_2), 1.41 (t, 3H, J = 7.2 Hz, CH_3). ^{13}C NMR (75 MHz, DMSO-d6) δ 166.0, 154.0, 149.2, 142.8, 135.9, 133.3, 132.5, 131.0, 130.0, 126.5, 126.1, 122.7 (2 × C), 115.8 (2 × C), 62.7, 14.5.

*5.2.8. Ethyl 3-((4-((tert-butoxycarbonyl)amino)phenyl)amino) quinoxaline-2-carboxylate (**4f**)*

The title compound was synthesized according to the general method A from compound **3** (95 mg, 0.40 mmol), *tert*-butyl (4-aminophenyl)carbamate (250 mg, 1.20 mmol) in absolute ethanol (6.5 mL). The reaction mixture was refluxed for 64 h in a sealed tube. After purification by silica column chromatography using CH_2Cl_2 with MeOH gradient (0–2%) as eluent, compound **4f** was obtained (152 mg, 93%) as an orange powder.

Mp 198.1 °C. ^{1}H NMR (300 MHz, DMSO-d6) δ 10.00 (bs, 1H, NH), 9.35 (bs, 1H, NH), 8.00–7.40 (m, 8H), 4.48 (q, 2H, J = 7.2 Hz, CH_2), 1.49 (s, 9H, 3 × CH_3), 1.41 (t, 3H, J = 7.2 Hz, CH_3CH_2O).

*5.2.9. Ethyl 3-((4-aminophenyl)amino)quinoxaline-2-carboxylate (**4g**)*

To a solution of compound **4f** (37 mg, 0.09 mmol) in CH_2Cl_2 (5 mL) was added dropwise trifluoroacetic acid (1 mL, 13.06 mmol). The mixture was stirred at room temperature for 6 h. The resulting mixture was made alkaline with a saturated sodium carbonate solution and extracted with CH_2Cl_2. The combined organic layers were dried over $MgSO_4$, filtered, and evaporated under reduced pressure to give the desired derivative **4g** (27 mg, 96%) as a red powder.

Mp 203.3 °C. ^{1}H NMR (300 MHz, $CDCl_3$) δ 10.06 (bs, 1H, NH), 8.01 (dd, 1H, J = 8.4, 1.2 Hz), 7.80–7.64 (m, 4H), 7.44 (dd, 1H, J = 8.1, 6.6, 1.2 Hz), 6.77 (d, 2H, J = 8.7 Hz), 4.61 (q, 2H, J = 7.2 Hz, CH_2), 3.70 (bs, 2H, NH_2), 1.55 (t, 3H, J = 7.2 Hz, CH_3). ^{13}C NMR (75 MHz, $CDCl_3$) δ 166.4, 149.7, 143.6, 142.6, 136.2, 132.8, 130.6, 130.5, 130.2, 126.6, 125.4, 122.4 (2 × C), 115.5 (2 × C), 62.9, 14.3.

*5.2.10. Ethyl 3-((4-(1-methylpiperidin-4-yl)phenyl)amino) quinoxaline-2-carboxylate (**4h**)*

The title compound was synthesized according to the general method A from compound **3** (45 mg, 0.19 mmol) and 4-(1-methylpiperidin-4-yl)aniline (40 mg, 0.21 mmol) in absolute ethanol (1.5 mL). The reaction mixture was refluxed for 112 h. After purification by silica column chromatography using CH_2Cl_2 with MeOH gradient (0–10%) as eluent, compound **4h** was obtained (47 mg, 63%) as an orange powder.

Mp 127 °C. ^{1}H NMR (300 MHz, $CDCl_3$) δ 10.28 (bs, 1H, NH), 8.02 (dd, 1H, J = 8.1, 1.2 Hz), 7.84 (d, 2H, J = 8.4 Hz), 7.77 (dd, 1H, J = 8.1, 1.2 Hz), 7.69 (dd, 1H, J = 8.1, 6.6, 1.2 Hz), 7.47 (dd, 1H, J = 8.1, 6.6, 1.2 Hz), 7.26 (d, 2H, J = 8.4 Hz), 4.59 (q, 2H, J = 7.2 Hz, CH_2), 3.30 (d, 2H, J = 11.7 Hz), 2.70–2.45 (m, 6H), 2.24–2.09 (m, 2H), 1.96 (d, 2H, J = 11.7 Hz), 1.53 (t, 3H, J = 7.2 Hz, CH_3). ^{13}C NMR (75 MHz, $CDCl_3$) δ 166.4, 149.3, 143.2, 139.4, 137.7, 136.4, 132.9, 130.5, 130.2, 127.3 (2 × C), 126.7, 125.9, 120.5 (2 × C), 63.0, 55.7 (2 × C), 45.1, 40.4, 31.9 (2 × C), 14.3.

*5.2.11. Ethyl 3-((2-hydroxyphenyl)amino)quinoxaline-2-carboxylate (**4i**)*

The title compound was synthesized according to the general method A from compound **3** (239 mg, 1.01 mmol) and 2-aminophenol (121 mg, 1.11 mmol) in absolute ethanol (10 mL). The reaction mixture was refluxed for 110 h. Compound **4i** was obtained (156 mg, 50%) as an orange powder.

Mp 166.6 °C. ^{1}H NMR (300 MHz, DMSO-d6) δ 10.66 (bs, 1H, NH), 10.16 (bs, 1H, OH), 8.89 (m, 1H), 7.99 (d, 1H, J = 8.1 Hz), 7.80 (m, 2H), 7.56 (m, 1H), 7.00–6.82 (m, 3H), 4.49 (q, 2H, J = 7.2 Hz, CH_2), 1.43 (t, 3H, J = 7.2 Hz, CH_3). ^{13}C NMR (75 MHz, DMSO-d6) δ 165.8, 149.0, 147.0, 142.6, 135.9, 133.5, 132.3, 130.1, 128.4, 126.6, 126.5, 123.1, 119.7, 119.6, 114.7, 62.7, 14.6.

*5.2.12. 3-((3-Hydroxyphenyl)amino)quinoxaline-2-carboxylic acid (**1**)*

Method B: to ester **4a** (72 mg, 0.23 mmol) in aqueous methanol (80%, 10 mL), was added potassium carbonate (97 mg, 0.70 mmol) and the reaction mixture was refluxed for 4 h. After cooling, the solvent was removed under reduced pressure. Then, the residue was acidified with a saturated citric acid aqueous solution, and extracted with ethyl acetate. The combined organic layers were dried over $MgSO_4$, filtered, and evaporated under reduced pressure to yield the acid **1** (33 mg, 50%) as a red powder.

Mp 199.6 °C. ^{1}H NMR (300 MHz, DMSO-d6) δ 10.52 (bs, 1H, NH), 9.51 (bs, 1H, OH), 7.98 (d, 1H, J = 8.4 Hz), 7.84–7.76 (m, 2H), 7.60–7.54 (m, 2H), 7.25–7.14 (m, 2H), 6.50 (d, 1H, J = 7.8 Hz). ^{13}C NMR (75 MHz, DMSO-d6) δ 168.1, 158.3, 149.3, 142.5, 140.7, 136.0, 133.2, 132.9, 130.1, 130.0, 126.6, 126.5, 111.0, 110.5, 107.2. HRMS (ESI) m/z: $[M+H]^+$ calcd for $C_{15}H_{12}N_3O_3$, 282.2742; found, 282.0873.

*5.2.13. Potassium 3-((3-aminophenyl)amino)quinoxaline-2-carboxylate (**5b**)*

Method C: to ester **4b** (82 mg, 0.26 mmol) in aqueous methanol (80%, 10 mL) was added potassium carbonate (37 mg, 0.26 mmol), and the reaction mixture was refluxed for 4 h. After cooling, the solvent was removed under reduced pressure, and freeze-dried to obtain compound **5b** (84 mg, 100%) as an orange powder.

Mp > 375 °C. ^{1}H NMR (300 MHz, DMSO-d6) δ 13.15 (bs, 1H, NH), 7.82 (dd, 1H, J = 8.4, 1.5 Hz), 7.65 (dd, 1H, J = 7.2, 1.8 Hz), 7.58 (td, 1H, J = 7.2, 1.5 Hz), 7.38 (dd, 1H, J = 8.4, 7.2, 1.8 Hz), 7.21 (t, 1H, J = 1.8 Hz), 7.14 (dd, 1H, J = 7.8, 1.8 Hz), 6.97 (t, 1H, J = 7.8 Hz), 6.22 (dd, 1H, J = 7.8, 1.8 Hz), 5.04 (bs, 2H, NH_2). ^{13}C NMR (75 MHz, DMSO-d6) δ 166.7, 150.4, 149.6, 143.2, 141.6, 141.5, 136.6, 130.2, 129.5 (2 × C), 125.9, 124.4, 108.5, 107.5, 104.9. HRMS (ESI) m/z: $[M+H]^+$ calcd for $C_{15}H_{13}N_4O_2$, 281.2895; found, 281.1032.

*5.2.14. 3-((3-Morpholinophenyl)amino)quinoxaline-2-carboxylic acid (**5c**)*

The title compound was synthesized according to the general method B from compound **4c** (150 mg, 0.40 mmol) and potassium carbonate (218 mg, 1.58 mmol) in aqueous methanol (80%, 5 mL).

The reaction mixture was refluxed for 4 h. Compound **5c** was obtained (139 mg, 100%) as an orange powder.

Mp 186.6 °C. ^{1}H NMR (300 MHz, DMSO-d6) δ 10.49 (bs, 1H, NH), 7.97 (m, 1H), 7.82–7.74 (m, 2H), 7.67 (s, 1H), 7.56 (dd, 1H, J = 8.4, 6.3, 2.1 Hz) 7.32 (d, 1H, J = 8.7 Hz), 7.23 (t, 1H, J = 8.1 Hz), 6.69 (dd, 1H, J = 8.1, 1.5 Hz), 3.77 (m, 4H, 2 × CH_2O morpholine), 3.16 (m, 4H, 2 × CH_2N, morpholine). ^{13}C NMR (75 MHz, DMSO-d6) δ 168.0, 152.2, 149.4, 142.5, 140.5, 135.9, 133.2, 132.9, 129.9, 129.7, 126.7, 126.4, 111.4, 110.5, 106.9, 66.6 (2 × C), 49.0 (2 × C). HRMS (ESI) m/z: $[M+H]^+$ calcd for $C_{19}H_{19}N_4O_3$, 351.3793; found, 351.1453.

5.2.15. 3-((1H-indol-5-yl)amino)quinoxaline-2-carboxylic acid (**5d**)

To ester **4d** (81 mg, 0.24 mmol) in ethanol (5 mL), was added a 10% sodium hydroxide solution (2 mL) and the reaction mixture was refluxed for 18 h. Ethanol was then evaporated under reduced pressure, and the resulting residue was acidified to pH 2 with a 15% citric acid solution and extracted with ethyl acetate. The organic layers were then washed with water and brine, dried over $MgSO_4$, filtered, and evaporated under reduced pressure. The residue was finally purified by silica column chromatography using CH_2Cl_2 with MeOH gradient (0–20%) as eluent to give the acid **5d** (30 mg, 41%) as a red powder.

Mp 244.4 °C. ^{1}H NMR (300 MHz, DMSO-d6) δ 12.45 (bs, 1H, NH), 11.07 (bs, 1H, NH), 8.70–6.80 (m, 8H), 6.44 (bs, 1H, indolyl). ^{13}C NMR (75 MHz, DMSO-d6) δ 168.6, 151.4, 133.6, 133.1, 132.5, 129.9, 129.4, 129.1 (3 × C), 127.1, 126.9, 125.7, 116.6, 112.9, 111.6, 102.5. HRMS (ESI) m/z: $[M+H]^+$ calcd for $C_{17}H_{13}N_4O_2$, 305.3109; found, 305.1034.

5.2.16. 3-((4-Hydroxyphenyl)amino)quinoxaline-2-carboxylic acid (**5e**)

The title compound was synthesized according to the general method B from compound **4e** (90 mg, 0.29 mmol) and potassium carbonate (80 mg, 0.58 mmol) in aqueous methanol (80%, 10 mL). The reaction mixture was refluxed for 4 h. Compound **5e** was obtained (79 mg, 97%) as an orange powder.

Mp 197.4 °C. ^{1}H NMR (300 MHz, DMSO-d6) δ 10.22 (bs, 1H, NH), 9.31 (bs, 1H, OH), 7.93 (dd, 1H, J = 8.1, 0.9 Hz), 7.78–7.63 (m, 4H), 7.51 (dd, 1H, J = 8.1, 6.6, 1.5 Hz), 6.80 (d, 2H, J = 8.7 Hz). ^{13}C NMR (75 MHz, DMSO-d6) δ 168.1, 153.9, 149.6, 142.9, 135.8, 133.2, 132.7, 131.1, 129.9, 126.4, 125.9, 122.5 (2 × C), 115.8 (2 × C). HRMS (ESI) m/z: $[M+H]^+$ calcd for $C_{15}H_{12}N_3O_3$, 282.2742; found, 282.0873.

5.2.17. Potassium 3-((4-aminophenyl)amino)quinoxaline-2-carboxylate (**5g**)

The title compound was synthesized according to the general method C from compound **4g** (16 mg, 0.05 mmol) and potassium carbonate (7 mg, 0.05 mmol) in aqueous methanol (80%, 5 mL). The reaction mixture was refluxed for 4 h. Compound **5g** was obtained (14 mg, 87%) as a red powder.

Mp > 375 °C. ^{1}H NMR (300 MHz, DMSO-d6) δ 12.80 (bs, 1H, NH), 7.84 (d, 1H, J = 7.8 Hz), 7.60–7.50 (m, 4H), 7.32 (m, 1H), 6.60 (d, 2H, J = 8.4 Hz), 4.84 (bs, 2H NH_2). ^{13}C NMR (75 MHz, DMSO-d6) δ 167.0, 150.4, 144.2, 143.0, 142.0, 136.4, 130.4, 130.2, 129.5, 125.6, 123.8, 120.9 (2 × C), 114.7 (2 × C). HRMS (ESI) m/z: $[M+H]^+$ calcd for $C_{15}H_{13}N_4O_2$, 281.2895; found, 281.1032.

5.2.18. 3-((4-(1-Methylpiperidin-4-yl)phenyl)amino)quinoxaline-2-carboxylic acid (**5h**)

The title compound was synthesized according to the general method B from compound **4h** (42 mg, 0.11 mmol) and potassium carbonate (45 mg, 0.32 mmol) in aqueous methanol (80%, 5 mL). The reaction mixture was refluxed for 4 h. Compound **5h** was obtained (19 mg, 49%) as a yellow powder.

Mp 321 °C. ^{1}H NMR (300 MHz, DMSO-d6) δ 13.33 (bs, 1H, NH), 8.00 (d, 1H, J = 7.8 Hz), 7.85 (d, 2H, J = 8.4 Hz), 7.68–7.58 (m, 2H), 7.54–7.31 (m, 1H), 7.23 (d, 2H, J = 8.4 Hz), 2.86 (d, 2H, J = 11.4 Hz), 2.46–2.36 (m, 1H), 2.19 (s, 3H, CH_3), 1.95 (td, 2H, J = 11.4, 1.8 Hz), 1.77–1.62 (m, 4H). ^{13}C NMR (75 MHz, DMSO-d6) δ 166.9, 150.4, 142.1, 141.7, 140.1, 138.8, 136.4, 130.7, 129.8, 127.5 (2 × C), 125.9, 124.7, 119.3 (2 × C), 56.4 (2 × C), 46.7, 41.2, 33.7 (2 × C). HRMS (ESI) m/z: an abundant fragment ion has been observed at m/z 213.1022 that have been attributed to the loss of the 1-methylpiperidin-4-yl) phenyl)amino moiety from the quinoxaline ring to form the ion $[C_9H_6N_2O_2 + K]^+$ (m/z calcd for $C_9H_6KN_2O_2$, 213.2545; found, 213.1022).

5.2.19. 3-((2-Hydroxyphenyl)amino)quinoxaline-2-carboxylic acid (**5i**)

The title compound was synthesized according to the general method B from compound **4i** (101 mg, 0.33 mmol) and potassium carbonate (135 mg, 0.98 mmol) in aqueous methanol (80%, 10 mL). The reaction mixture was refluxed for 4 h. Compound **5i** was obtained (60 mg, 65%) as a red powder.

Mp 191.1 °C. ^{1}H NMR (300 MHz, DMSO-d6) δ 14.00 (bs, 1H, COOH), 10.84 (bs, 1H, NH), 10.11 (bs, 1H, OH), 8.88 (m, 1H), 7.97 (d, 1H, J = 8.1 Hz), 7.80 (m, 2H), 7.56 (m, 1H), 7.00–6.68 (m, 3H). ^{13}C NMR (75 MHz, DMSO-d6) δ 167.1, 148.7, 146.5, 142.2, 135.3, 132.7, 132.4, 129.4, 127.9, 126.1, 125.8, 122.5, 119.2, 119.0, 114.2. HRMS (ESI) m/z: $[M+H]^+$ calcd for $C_{15}H_{12}N_3O_3$, 282.2742; found, 282.0871.

5.2.20. 3-((3-Morpholinophenyl)amino)quinoxaline-2-carboxamide (**6**)

To a solution of compound **5c** (50 mg, 0.14 mmol) and *N*-methylmorpholine (31 μL, 0.29 mmol) in dichloromethane (5 mL) at 0 °C, was added ethyl chloroformate (21 μL, 0.21 mmol). The reaction mixture was stirred magnetically at 0 °C for 1 h, and a 28% solution of ammonium hydroxide (5 mL) was added. The reaction was stirred overnight at room temperature and extracted with dichloromethane. The organic layer was then washed with water and brine, dried over $MgSO_4$, filtered, and evaporated under reduced pressure to give the carboxamide **6** (50 mg, 100%) as a red powder.

Mp 203.9 °C. ^{1}H NMR (300 MHz, DMSO-d6) δ 11.52 (bs, 1H, NH), 8.75 (bs, 1H, NH_2), 8.26 (bs, 1H, NH_2), 7.93 (d, 1H, J = 8.1 Hz), 7.82–7.50 (m, 2H), 7.69 (bs, 1H), 7.56 (m, 1H), 7.32–7.20 (m, 2H), 6.69 (d, 1H, J = 8.1 Hz), 3.78 (m, 4H, 2 × CH_2O morpholine), 3.17 (m, 4H, 2 × CH_2N, morpholine). ^{13}C NMR (75 MHz, DMSO-d6) δ 168.5, 152.2, 149.4, 142.7, 140.6, 135.3, 133.1, 132.8, 129.8, 129.6, 126.7, 126.3, 111.1, 110.3, 106.6, 66.6 (2 × C), 49.0 (2 × C). HRMS (ESI) m/z: $[M+H]^+$ calcd for $C_{19}H_{20}N_5O_2$, 350.3946; found, 350.1613.

5.3. Molecular modeling

Molecular modeling studies were performed using SYBYL-X 1.3 software [33] running on a Dell precision T3400 workstation. The three-dimensional structure of compound **1** (under its carboxylate form to imitate physiological conditions) was built from a standard fragments library and optimized using the Tripos force field [34] including the electrostatic term calculated from Gasteiger and Hückel atomic charges. Powell's method available in Maximin2 procedure was used for energy minimization until the gradient value was smaller than 0.001 kcal/(mol*Å). The crystal structure of Pim-1 in complex with AMP-PNP at 1.6 Å resolution (PDB ID 3A99) [35] was used as template for docking. Water molecules were removed from the coordinates set since no information about conserved water molecules is known for this chemical series in Pim-1. Flexible docking of compound **1** into ATP-binding site was performed using GOLD software [36]. The most stable docking

model was selected according to the best scored conformation predicted by the GoldScore scoring function. Finally, the complex was energy-minimized using Powell's method available in Maximin2 procedure with the Tripos force field and a dielectric constant of 4.0, until the gradient value reached 0.1 kcal/mol.Å.

5.4. Biology

5.4.1. Mammalian protein kinase assays

Kinase enzymatic activities were assayed in 384-well plates using the ADP-Glo™ assay kit (Promega, Madison, WI) according to the recommendations of the manufacturer. This assay is a luminescent ADP detection assay that provides a homogeneous and high-throughput screening method to measure kinase activity by quantifying the amount of ADP produced during a kinase reaction. Briefly, the reactions were carried out in a final volume of 5 μL for 30 min at 30 °C in ADP-Glo buffer and 10 μM ATP (40 mM Tris pH 7.5, 20 mM $MgCl_2$ and 0.1 mg/mL of BSA). After that, 5 μL of ADP-Glo™ Kinase Reagent was added to stop the kinase reaction. After an incubation time of 50 min at room temperature (rt), 10 μL of Kinase Detection Reagent was added for 1 h at rt. The transmitted signal was measured using the Envision (PerkinElmer, Waltham, MA) microplate luminometer and expressed in Relative Light Unit (RLU). In order to determine the half maximal inhibitory concentration (IC_{50}), the assays were performed in triplicate in the absence or presence of increasing doses of the tested compounds. Kinase activities are expressed in % of maximal activity, *i.e.* measured in the absence of inhibitor. Peptide substrates were obtained from Proteogenix (Schiltigheim, France).

The following kinases were analyzed during this study: *Hs*Pim-1 (human proto-oncogene, recombinant, expressed in bacteria) was assayed with 0.8 μg/μL of histone H1 (Sigma #H5505) as substrate; *Rn*DYRK1A-kd (*Rattus norvegicus*, amino acids 1 to 499 including the kinase domain, recombinant, expressed in bacteria, DNA vector kindly provided by Dr. W. Becker, Aachen, Germany) was assayed with 0.033 μg/μL of the following peptide: KKISGRLSPIMTEQ as substrate; *Hs*CDK2/CyclinA (cyclin-dependent kinase-2, human, kindly provided by Dr. A. Echalier-Glazer, Leicester, UK) was assayed with 0.8 μg/μL of histone H1 as substrate; *Hs*CDK9/CyclinT (human, recombinant, expressed by baculovirus in Sf9 insect cells) was assayed with 0.27 μg/μL of the following peptide: YSPTSPSYSPTSPSYSPTSPSKKKK, as substrate; *Hs*Haspin-kd (human, kinase domain, amino acids 470 to 798, recombinant, expressed in bacteria) was assayed with 0.007 μg/μL of Histone H3 (1–21) peptide (ARTKQTARKSTGGKAPRKQLA) as substrate; *Mm*CLK1 (from *Mus musculus*, recombinant, expressed in bacteria) was assayed with 0.027 μg/μL of the following peptide: GRSRSRSRSRSR as substrate; *Ssc*CK1δ/ε (casein kinase 1δ/ε, porcine brain, native, affinity purified) was assayed with 0.022 μg/μL of the following peptide: RRKHAAIGSpAYSITA ("Sp" stands for phosphorylated serine) as CK1-specific substrate; *Ssc*GSK-3α/β (glycogen synthase kinase-3, porcine brain, native, affinity purified) isoforms were assayed with 0.010 μg/μL of GS-1 peptide, a GSK-3-selective substrate (YRRAAVPPSPSLSRHSSPHQSpEDEEE). To validate the kinase assay, model inhibitors were used for each tested enzyme: Staurosporine from *Streptomyces* sp. (#S5921, purity ≥95%, Sigma-Aldrich) for *Ssc*CK1δ/ε; Indirubin-3′-oxime (#I0404, purity ≥98%, Sigma-Aldrich) for *Ssc*GSK-3α/β, *Hs*Pim-1, human Cyclin-dependent kinases, *Rn*DYRK1A and *Mm*CLK1; CHR-6494 (#SML0648, purity ≥98%, Sigma-Aldrich) for Haspin.

5.4.2. Cell cultures and reagents

KU812 cell lines were obtained from the American Type Culture Collection (ATCC) and maintained according to the supplier's recommendations. Cell lines were cultured in RPMI, with 10% fetal bovine serum, 1% glutamine, and 1% penicillin/streptomycin at 37 °C and 5% CO_2.

5.4.3. Cell proliferation assays

Cell viability and proliferation were studied using a MTT cell proliferation assay. Briefly, 0.2×10^5 cells were incubated in 100 μL of X-Vivo red phenol free medium (Lonza, Basel, Switzerland) in 96 well plates. In initial screening assays, cells were incubated with 10 μM of each compound (quinoxalines stock solution at 50 mM in DMSO) for 24, 48, and 72 h. Imatinib mesylate (Selleckchem, stock solution at 10 mM in DMSO) was used as reference. To determine the concentration-effect of the molecules, cells were treated with concentrations ranging from 100 nM to 50 μM for 24 or 48 h. Cells were incubated with 10 μL of MTT working solution (5 g/L of methylthiazolyldiphenyl-tetrazolium bromide) during 4 h. Cells were then lysed overnight at 37 °C with 100 μL of 10% SDS and 0.003% HCl. Optical density (OD) at 570 nm was measured using a spectrophotometer (Dynex, Chantilly, United States). Living cells were also counted with the trypan blue dye exclusion method. When a dose-dependent activity was observed, EC_{50} values were calculated using Graphpad PRISM 7 software ($n = 3$ in triplicate). Data were collected from at least three independent experiments and the values reported are means ± standard errors of the mean.

Acknowledgments

This work was supported by a grant from the « *Association pour le Développement de la Recherche et de l'Innovation dans le NORD PAS DE CALAIS* » (ADRINORD) (to B. O.). The authors thank the « *Plateforme Scientifique et Technique Analyses des Systèmes Biologiques* » (PST-ASB), Tours (France), for NMR spectrometry and the « *Fédération de Recherche* » ICOA/CBM (FR2708) platform, for HRMS analyses. The authors also thank the Cancéropôle Grand Ouest (axis: Natural sea products in cancer treatment), GIS IBiSA (*Infrastructures en Biologie Santé et Agronomie*) and Biogenouest (Western France life science and environment core facility network) for supporting KISS*f* screening facility. The authors wish to thank the *Région Centre Val de Loire* for financial support.

Appendix A. Supplementary data

Supplementary data related to this article can be found at https://doi.org/10.1016/j.ejmech.2018.04.056.

References

[1] H.T. Cuypers, G. Selten, W. Quint, M. Zijlstra, E.R. Maandag, W. Boelens, P. Van Wezenbeek, C. Melief, A. Berns, Murine leukemia virus-induced T-cell lymphomagenesis: integration of proviruses in a distinct chromosomal region, Cell 37 (1984) 141–150.
[2] T. Mochizuki, C. Kitanaka, K. Noguchi, T. Muramatsu, A. Asai, Y.J. Kuchino, Physical and functional interactions between Pim-1 kinase and Cdc25A phosphatase. Implications for the Pim-1-mediated activation of the c-Myc signaling pathway, J. Biol. Chem. 274 (1999) 18659–18666.
[3] M. Bachmann, C. Kosan, P.X. Xing, M. Montenarh, I. Hoffmann, T. Möröy, The oncogenic serine/threonine kinase Pim-1 directly phosphorylates and activates the G2/M specific phosphatase Cdc25C, Int, J. Biochem. Cell Biol. 38 (2006) 430–443.
[4] R. Amson, F. Sigaux, S. Przedborski, G. Flandrin, D. Givoland, A. Telerman, The human protooncogene product p33pim is expressed during fetal hematopoiesis and in diverse leukemias, Proc. Natl. Acad. Sci. U. S. A 86 (1989) 8857–8861.
[5] E.D. Hsi, S.H. Jung, R. Lai, J.L. Johnson, J.R. Cook, D. Jones, S. Devos, B.D. Cheson, L.E. Damon, J. Said, Ki67 and PIM1 expression predict outcome in mantle cell lymphoma treated with high dose therapy, stem cell transplantation and rituximab: a Cancer and Leukemia Group B 59909 correlative science study, Leuk. Lymphoma 49 (2008) 2081–2090.
[6] S.J. Guo, X.P. Mao, J.X. Chen, B. Huang, C. Jin, Z.B. Xu, S.P. Qiu, Overexpression of Pim-1 in bladder cancer, J. Exp. Clin. Canc. Res. 29 (2010) 161.
[7] S.M. Dhanasekaran, T.R. Barrette, D. Ghosh, R. Shah, S. Varambally, K. Kurachi,

K.J. Pienta, M.A. Rubin, A.M. Chinnaiyan, Delineation of prognostic biomarkers in prostate cancer, Nature 412 (2001) 822–826.
[8] F. Brasó-Maristany, S. Filosto, S. Catchpole, R. Marlow, J. Quist, E. Francesch-Domenech, D.A. Plumb, L. Zakka, P. Gazinska, G. Liccardi, P. Meier, A. Gris-Oliver, M.C. Cheang, A. Perdrix-Rosell, M. Shafat, E. Noël, N. Patel, K. McEachern, M. Scaltriti, P. Castel, F. Noor, R. Buus, S. Mathew, J. Watkins, V. Serra, P. Marra, A. Grigoriadis, A.N. Tutt, PIM1 kinase regulates cell death, tumor growth and chemotherapy response in triple-negative breast cancer, Nat. Med. 22 (2016) 1303–1313.
[9] B. Yan, E.X. Yau, S. Samanta, C.W. Ong, K.J. Yong, L.K. Ng, B. Bhattacharya, K.H. Lim, R. Soong, K.G. Yeoh, N. Deng, P. Tan, Y.L. Lam, M. Salto-Tellez, Clinical and therapeutic relevance of PIM1 kinase in gastric cancer, Gastric Cancer 15 (2012) 188–197.
[10] Y. Tursynbay, J. Zhang, Z. Li, T. Tokay, Z. Zhumadilov, D. Wu, Y. Xie, Pim-1 kinase as cancer drug target: an update, Biomed, For. Rep. 4 (2016) 140–146.
[11] H. Mikkers, M. Nawijn, J. Allen, C. Brouwers, E. Verhoeven, J. Jonkers, A. Berns, Mice deficient for all PIM kinases display reduced body size and impaired responses to hematopoietic growth factors, Mol. Cell Biol. 24 (2004) 6104–6115.
[12] R.A. Darby, A. Unsworth, S. Knapp, I.D. Kerr, R. Callaghan, Overcoming ABCG2-mediated drug resistance with imidazo-[1,2-*b*]-pyridazine-based Pim1 kinase inhibitors, Cancer Chemother, Pharmacology (Basel) 76 (2015) 853–864.
[13] Y. Xie, S. Bayakhmetov, PIM1 kinase as a promise of targeted therapy in prostate cancer stem cells, Mol. Clin. Oncol 4 (2016) 13–17.
[14] C. Liang, Y.Y. Li, Use of regulators and inhibitors of Pim-1, a serine/threonine kinase, for tumour therapy (review), Mol. Med. Rep. 9 (2014) 2051–2060.
[15] F. Anizon, A.A. Shtil, V.N. Danilenko, P. Moreau, Fighting tumor cell survival: advances in the design and evaluation of Pim inhibitors, Curr. Med. Chem. 17 (2010) 4114–4133.
[16] Y. Xu, B.G. Brenning, S.G. Kultgen, J.M. Foulks, A. Clifford, S. Lai, A. Chan, S. Merx, M.V. McCullar, S.B. Kanner, K.-K. Ho, Synthesis and biological evaluation of pyrazolo[1,5-*a*]pyrimidine compounds as potent and selective Pim-1 inhibitors, ACS Med. Chem. Lett. 6 (2015) 63–67.
[17] H.-B. Sun, X.-Y. Wang, G.-B. Li, L.-D. Zhang, J. Liu, L.-F. Zhao, Design, synthesis and biological evaluation of novel C3-functionalized oxindoles as potential Pim-1 kinase inhibitors, RSC Adv. 5 (2015) 29456–29466.
[18] C. Blanco-Aparicio, A. Carnero, Pim kinases in cancer: diagnostic, prognostic and treatment opportunities, Biochem. Pharmacol. 85 (2013) 629–643.
[19] A. Kumar, V. Mandiyan, Y. Suzuki, C. Zhang, J. Rice, J. Tsai, D.R. Artis, P. Ibrahim, R. Bremer, Crystal structures of proto-oncogene kinase Pim1: a target of aberrant somatic hypermutations in diffuse large cell lymphoma, J. Mol. Biol. 348 (2005) 183–193.
[20] B.T. Le, M. Kumarasiri, J.R. Adams, M. Yu, R. Milne, M.J. Sykes, S. Wang, Targeting Pim kinases for cancer treatment: opportunities and challenges, Future Med. Chem. 7 (2015) 35–53.
[21] L. Juen, M. Brachet-Botineau, C. Parmenon, J. Bourgeais, O. Hérault, F. Gouilleux, M.C. Viaud-Massuard, G. Prié, New inhibitor targeting signal transducer and activator of transcription 5 (STAT5) signaling in myeloid leukemias, J. Med. Chem. 60 (2017) 6119–6136.
[22] Z. Guo, A. Wang, W. Zhang, M. Levit, Q. Gao, C. Barberis, M. Tabart, J. Zhang, D. Hoffmann, D. Wiederschain, J. Rocnik, F. Sun, J. Murtie, C. Lengauer, S. Gross, B. Zhang, H. Cheng, V. Patel, L. Schio, F. Adrian, M. Dorsch, C. Garcia-Echeverria, S.M. Huang, PIM inhibitors target CD25-positive AML cells through concomitant suppression of STAT5 activation and degradation of MYC oncogene, Blood 124 (2014) 1777–1789.
[23] L.S. Chen, S. Redkar, D. Bearss, W.G. Wierda, V. Gandhi, Pim kinase inhibitor, SGI-1776, induces apoptosis in chronic lymphocytic leukemia cells, Blood 114 (2009) 4150–4157.
[24] Y. Xiang, B. Hirth, G. Asmussen, H.P. Biemann, K.A. Bishop, A. Good, M. Fitzgerald, T. Gladysheva, A. Jain, K. Jancsics, J. Liu, M. Metz, A. Papoulis, R. Skerlj, J.D. Stepp, R.R. Wei, The discovery of novel benzofuran-2-carboxylic acids as potent Pim-1 inhibitors, Bioorg. Med. Chem. Lett 21 (2011) 3050–3056.
[25] J. Bogusz, K. Zrubek, K.P. Rembacz, P. Grudnik, P. Golik, M. Romanowska, B. Wladyka, G. Dubin, Crystal structure of PIM1 kinase in complex with small-molecule inhibitor, Sci. Rep. 7 (2017), 13399–13399.
[26] R. Mahesh, A.K. Dhar, T. Sasank T. V. N. V, S. Thirunavukkarasu, T. Devadoss, Citric acid: an efficient and green catalyst for rapid one pot synthesis of quinoxaline derivatives at room temperature, Chin. Chem. Lett. 22 (2011) 389–392.
[27] R. Mahesh, T. Devadoss, A.K. Dhar, S.M. Venkatesh, S. Mundra, D.K. Pandey, S. Bhatt, A.K. Jindal, Ligand-based design, synthesis, and pharmacological evaluation of 3-methoxyquinoxalin-2-carboxamides as structurally novel serotonin type-3 receptor antagonists, Arch. Pharm. Chem. Life Sci. 345 (2012) 687–694.
[28] A. Kumar, K. Srivastava, S.R. Kumar, M.I. Siddiqi, S.K. Puri, J.K. Sexana, P.M. Chauhan, 4-Anilinoquinoline triazines: a novel class of hybrid antimalarial agents, Eur. J. Med. Chem. 46 (2011) 676–690.
[29] H. Zegzouti, M. Zdanovskaia, K. Hsiao, S.A. Goueli, ADP-Glo: a Bioluminescent and homogeneous ADP monitoring assay for kinases, Assay Drug Dev. Technol. 7 (2009) 560–572.
[30] P. Lassalas, B. Gay, C. Lasfargeas, M.J. James, V. Tran, K.G. Vijayendran, K.R. Brunden, M.C. Kozlowski, C.J. Thomas, A.B. Smith III, D.M. Huryn, C. Ballatore, Structure property relationships of carboxylic acid isosteres, J. Med. Chem. 59 (2016) 3183–3203.
[31] F. Jahani, M. Tajbakhsh, H. Golchoubian, S. Khaksar, Guanidine hydrochloride as an organocatalyst for N-Boc protection of amino groups, Tetrahedron Lett. 52 (2011) 1260–1264.
[32] R. Wurz, A. Tasker, S. Tadesse, L.H. Pettus, T.T. Nguyen, F.-T. Hong, B.J. Herberich, E. Harrington, J.J. Chen, J. Brown, Substituted 7-oxo-pyrido[2,3-*d*] pyrimidines and their use for the treatment of EGFR/ErbB2 related disorders, From PCT Int. Appl (2014) 108–109. WO2014134308.
[33] SYBYL-x 1.3, Tripos Associates, Inc, South Hanley Road, St. Louis, MO 63144, U.S.A, 1699.
[34] M. Clarck, R.D. Cramer III, N. Van Opdenbosch, Validation of the general purpose tripos 5.2 force field, J. Comput. Chem. 10 (1989) 982–1012.
[35] D. Morishita, M. Takami, S. Yoshikawa, R. Katayama, S. Sato, N. Kukimoto-Niino, T. Umehara, M. Shirouzu, K. Sekimizu, S. Yokoyama, N. Fujita, Cell-permeable carboxyl-terminal $p27^{Kip1}$ peptide exhibits anti-tumor activity by inhibiting Pim-1 kinase, J. Biol. Chem. 286 (2011) 2681–2688.
[36] G. Jones, P. Willet, R.C. Glen, Development and validation of a genetic algorithm for flexible docking, J. Mol. Biol. 267 (1997) 727–748.